Particulate measurement methods

Smallwood, Gregory J.; Bachalo, William D.; Sankar, Subramanian V.

Optical Metrology for Fluids Combustion and Solids, pp. 221-257, 2003

on, R.K., "Scanned- and fixed-measurements using multiplexed

S.T., Edwards, D.P., Flaud, J.-M., -Y., Schroeder, J., Mecann, A., , K.V., Jucks, K.W., Brown, L.R., cular spectroscopic database and edition," *Journal of Quantitative* 10.

water vapor concentration and s," *AIAA Journal* 34 (1996): 483–

ength-modulation spectroscopy for e, and velocity in shock-heated

ser-based air mass flux sensor for 96): 4905–4912.

ode laser sensor for gasdynamic *ournal* 38 (2000): 1246–1252.

W.J., Otis, C.E., Palombo, D.A., orption and gain spectroscopy: nsors," *Applied Optics* 34 (1995):

rt, H., Wolfrum, J., and Jaritz, H., election of Multiple Species and *h. Inst* 28 (2000): 423-430.

, M., "Tunable diode laser sensor esented at the 41st Conference of

macht, C., and Capasso, F., using room-temperature, mid-IR 0th AIAA Aerospace Sciences

Chapter 8

PARTICULATE MEASUREMENT METHODS

Gregory J. Smallwood,* William D. Bachalo,† and Subramanian V. Sankar†
*National Research Council, Canada, †Artium Technologies, Inc.

1. INTRODUCTION

The presence of soot is essential in some processes: it is the product in carbon black; it provides the source of light radiation in pyrotechnic and pyrophoric flares; and is the dominant source of radiant heat transfer in boilers and furnaces. However, it is also an undesirable product in many combustion processes where it is expelled with the exhaust, contributing to air pollution. The focus of this chapter is on measurement of the unwanted particulates, primarily from diesel, gasoline, and gas turbine engines, although the techniques described in most cases are equally effective in measuring soot in flames and from non-engine sources.

Particulate matter (PM) emissions from combustion processes can be comprised of both solid and volatile matter. The solid fraction consists primarily of elemental carbon (soot), but may also contain ash (metal sulfates and oxides). The occurrence of soot is the result of incomplete oxidation of the fuel, and appears as near-spherical primary particles that cluster to form aggregates, as shown in figure 1. The ash in PM emissions from engines is mostly from additives in the lubricating oil, but there are also metal oxides from engine wear and corrosion of exhaust system components. The volatile matter is mostly hydrocarbon from the fuel and lubricant, and hydrated sulfuric acid, and is found either adsorbed on the surface of solid particles, or in the form of small droplets no larger than the primary soot particles, where the latter are typically on the order of 20 to 50 nm in diameter.

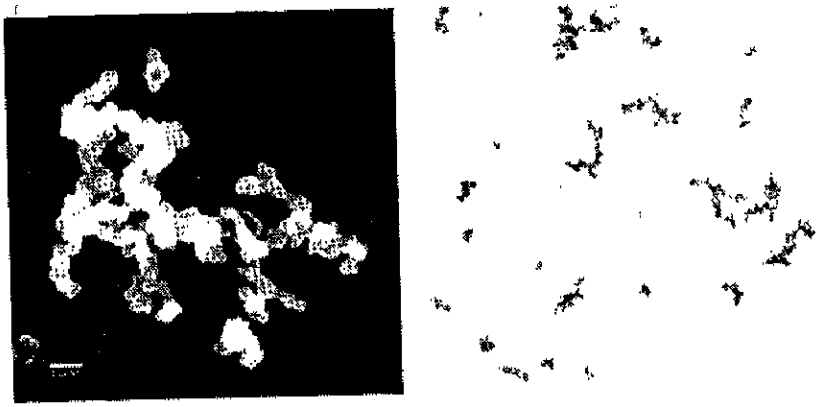

Figure 1. SEM (scanning electron microscope) image (left) and TEM (transmission electron microscope) image (right) of soot collected from a flame by thermophoretic sampling. A movie, *Ch8FlameSampling.avi* (included on CD,) illustrates thermophoretic sampling in a laminar flame.

1.1 Air Quality and Health Effects

Recent studies of the health effects of air pollution show that the levels of soot and other tiny particles found in large and midsize cities increase the risk of premature death from cancer and heart disease. Breathing high concentrations of lung-penetrating particulates has been shown by Arden et al.[1] to be an important environmental risk factor for cardiopulmonary and lung cancer mortality. Studies by the American Cancer Society concluded that as the concentration of soot particulates increases, the risk of early death rises by 4 to 8 percent and increases the number of aggravated asthma cases, depending on the concentration and long-term exposure. Fortunately, soot particulates emitted by cars, trucks, power plants, factories, aircraft, and other combustion processes have been reduced substantially over the past decade and will drop further under pending regulations. However certain regions undergoing rapid industrial development are producing higher levels of particulate emissions. These emissions travel on the jet stream to produce a global rather than simply a national or urban problem. Not only the mass of the particulates but also the size and number density play a significant role in the health effects on humans and other living organisms as well as upon the climate.

Efforts have focused on reducing the mass of the combustion-generated particulates in the larger PM_{10} size range (particulates below 10 μm aerodynamic diameter) which were visible and hence, readily associated with emissions at the source. However, especially deleterious are the small

sized respirable aerosols a
adverse health effects and
which adversely affect the
2.5 μm aerodynamic diam
the regulatory standard
regulations may be establi
0.3 μm size range deposit i
their way into the alveoli.
evidence indicates that th
emissions data show that
0.1 μm. However, it is th
dominate the mass-weighte

1.2 Regulations

Demand for improved
restrictive emission regu
America, and Japan. Prop
emissions levels will cont
currently regulated only fo
for all light duty vehicle
health concerns, there is
particulates in the exhaus
performance of the power

Growing environmer
requirements of diesel-pc
throughout Europe, North
of particulate emissions. T
restrictions on off-road
equipment will be impl
stationary sources and off
a trivial one since diesel-p
required in the transporta
operations and to consum
burn technologies (diese
produce more particulates
emissions control systems
reduce pollutant formatio
adequate performance of

Currently, particle size
regulated. At least two fa

instrumentation to adequately characterize the size and number of fine amorphous particulates; and the general lack of medical research evidence to define acceptable levels of PM as a function of aggregate size. However, the recent research cited above indicates that particulate levels existing in urban areas are producing significant hazards to our health. Furthermore, instrumentation developments are progressing that will allow more reliable and convenient means for characterizing the particulates that will lead to improved correlations between particulate loading and expression of deleterious health effects.

To develop processes and techniques for limiting the emission of soot, we must first possess suitable means for reliably measuring various soot-related parameters. These methods must have adequate measurement range in order to monitor and characterize the pollutant emissions over a very wide range of concentrations, and must operate under a range of environmental conditions from *in situ* exhaust to atmospheric monitoring. In the case of particulate matter, information on the particle mass, size, and volume fraction is needed. The lack of availability of suitable diagnostics has resulted in a degree of uncertainty in the correlation of the particulate loading with health effects. Improvements in the instrumentation are needed to help in developing the test protocols, standards and regulations that will preserve the environment and limit risks to health. Laser-induced incandescence (LII) has emerged as a technique for measuring soot concentration and size, as it appears that non-soot matter is evaporated and/or does not contribute to the signal.

1.3 Characteristics of Particulate Emissions

Particulates present challenging measurement problems, both in determining the appropriate quantity to be measured and the technique to perform the measurement. Due to the aggregate morphology and often complex composition of PM these nonspherical particles are difficult to characterize as there are many parameters to specify. As an example, the size of the aggregate can be characterized by the number of primary particles in the aggregate, the diameter of a sphere with equivalent bulk material volume, the Feret diameter, the aerodynamic diameter, and the mobility diameter.

One common characteristic is that there is typically a high number density of particulates (10^5 to 10^{10} particles/cm^3) even when the total volume concentration is relatively low so that particle counting techniques often require the flow to be diluted until the number density is within the range of the instrument. The range of loading is very wide, ranging from volume

concentrations of <0.1 ppt for
to >10 ppm for in-flame or ca
8 orders of magnitude.

Soot formation occurs i
growth of the individual pri
aggregation. The aggregatior
number density of particles. T
to aggregation and decreasi
soot exits regions with tempe
formation and oxidation rea
The aggregates are mass-fr
aggregate follows a fractal-li

In engine exhaust the
hydrocarbons and other com
soot particles. The contribut
significantly reduced in the
into effect. However, it will
lubricating oil is likely to re
by UV radiation, further ch
with other species in the atn
mass is unknown *a prior*
composition of the particulat

1.4 Associated Me

Currently, in terms of
diesel engines are defined
from a dilute exhaust stre
excludes condensed water t
this temperature or above.
emissions data for the peric
the filter. Transient PM me
Agglomeration of the colle
the filter so the measuremer
be possible. Furthermore,
generated is reduced, whic
reproducibility and sensitiv
the future.

Concerns regarding th
temperature, preconditioni

concentrations of <0.1 ppt for smog-free ambient atmospheric measurements to >10 ppm for in-flame or carbon black reactor measurements—greater than 8 orders of magnitude.

Soot formation occurs in flames via nucleation of primary particles, growth of the individual primary particles, and collisions leading to rapid aggregation. The aggregation process leads to a significant reduction in the number density of particles. The particle size changes rapidly, increasing due to aggregation and decreasing due to oxidation of the particles. Once the soot exits regions with temperatures and conditions sufficient to maintain the formation and oxidation reactions, the soot volume concentration is fixed. The aggregates are mass-fractals as the number of primary particles per aggregate follows a fractal-like behavior.

In engine exhaust there can be significant levels of unburned hydrocarbons and other combustion byproducts which can condense on the soot particles. The contribution from hydrated sulfuric acid is likely to be significantly reduced in the near future as low sulfur fuel regulations come into effect. However, it will not disappear completely as the sulfur content in lubricating oil is likely to remain high for the foreseeable future. Stimulated by UV radiation, further changes occur after emission as the particles react with other species in the atmosphere. The relation between particle size and mass is unknown *a priori*, due to the variations in morphology and composition of the particulates.

1.4 Associated Measurement Problems

Currently, in terms of monitoring, particulate matter emissions from diesel engines are defined as the mass of the matter that can be collected from a dilute exhaust stream on a filter kept below 52°C. The method excludes condensed water but includes organic compounds that condense at this temperature or above. These measurements provide time-average PM emissions data for the period during which the particulates are collected on the filter. Transient PM measurements using this technique are impractical. Agglomeration of the collected PM and other condensed material occurs on the filter so the measurement of particulate size and size distribution may not be possible. Furthermore, as diesel engines improve, the quantity of PM generated is reduced, which pushes this gravimetric technique closer to its reproducibility and sensitivity limits, limiting it to one of marginal utility for the future.

Concerns regarding the influence of dilution ratio, residence time, temperature, preconditioning, and sampling line materials, as well as the

instruments to measure particulates are being voiced with increasing frequency. Many of the issues have been recently summarized by Witze.[5]

The differences in measured particulate size distributions and/or mass due to the sampling issues are attributed to marked variations in the quantity of condensed aerosols. It is generally accepted that the measurement of soot is insensitive to the sampling conditions. Recent evidence has indicated that soot emissions have characteristic size distributions which could be used to distinguish them from other aerosols.[6]

2. MEASUREMENT METHODS

2.1 Desirable Characteristic Measurements

The parameters of most interest in characterizing particulates are the mass concentration; volume concentration; number density; aggregate size; aggregate size distribution; active surface area; and composition.

2.2 Commonly Available Characteristic Measurements

An average mass concentration of particulates can be determined by the gravimetric filter method, and an average volume concentration can be determined by light extinction techniques. The number concentration can be determined by particle counting techniques up to about 10^5 to 10^7 particles/cm^3. There are instruments available to determine the aerodynamic and mobility diameters, and it is possible to measure a representative distribution of the mobility diameter.

There currently are no satisfactory *in situ* or online sampling methods for determining active surface area, which has significant health impacts as it provides the delivery mechanism for toxics, and is also important in determining performance of carbon black. Similarly, methods for determining composition are *ex situ* and offer poor reproducibility.

2.3 Overview of Available Instruments

For mass concentration measurements, the standard gravimetric filter technique is nearing its reproducibility and sensitivity limits with modern low emission engines, and it does not offer transient measurement capability. The tapered element oscillating microbalance (TEOM®) is another gravimetric method that does have a transient capability, but has similar

sensitivity limits, as it is measurable change in the

Volume concentration methods, provided the distribution of particles length of the path is kno counting instruments suc as the criterion of a sin limiting the upper co employed to determine t signals is greatly simplif spherical particles. Unfo interaction with light tha particles further complic likely to be present in th be used to achieve sin detecting small particles

There are several distributions. The aerody the electrical low press anomalies due to particl lack of sensitivity at lov distribution rapidly, al mobility diameter can b (SMPS) which provides SMPS for PM measur measurements. the effe mobility diameter,[7] mult in smaller size bins, and

Active surface area including the epiphanio aerosol sensor. These ultraviolet light, respect is proportional to the dependent upon the spectroscopy (ATOFM composition of the parti difficult to obtain repres

This overview of a details on these method that by Witze[5] and ref methods, such as lir

sensitivity limits, as it is limited by the change in mass necessary to create a measurable change in the frequency of oscillation.

Volume concentration can be determined by line-of-sight light extinction methods, provided the refractive index of the particles is known, the distribution of particles along the measurement path is uniform, and the length of the path is known. Number density can be determined by particle counting instruments such as the condensation nuclei counter (CNC) as long as the criterion of a single particle in the probe volume can be met, thus limiting the upper concentration. Light scattering methods are often employed to determine the particle size but the interpretation applied to the signals is greatly simplified as Mie (or Rayleigh) scattering theory assumes spherical particles. Unfortunately, the aggregates have a much more complex interaction with light than Mie theory provides. The high number density of particles further complicates scattering, as a distribution of particle sizes is likely to be present in the probe volume at any given moment. Dilution can be used to achieve single particle scattering, but then issues arise with detecting small particles due to weak signals.

There are several types of instruments available to measure size distributions. The aerodynamic diameter distribution can be determined with the electrical low pressure cascade impactor (ELPI). Although it suffers anomalies due to particle bounce, the need to correct the largest sizes, and a lack of sensitivity at low concentrations, it does provide a relatively coarse distribution rapidly, allowing transient distribution measurements. The mobility diameter can be measured with the scanning mobility particle sizer (SMPS) which provides a high resolution size distribution. Issues with the SMPS for PM measurements include that it is too slow for transient measurements, the effective density of the particle is a function of the mobility diameter,[7] multiple charge effects causing larger particles to appear in smaller size bins, and limits on the maximum number density of particles.

Active surface area can be measured by a variety of instruments, including the epiphaniometer, the diffusion charger, and the photoelectric aerosol sensor. These use radioactive isotopes, corona discharge, and ultraviolet light, respectively, to charge the particles. In all cases, the charge is proportional to the surface area, although in the latter case it is also dependent upon the particle composition. Atomic time-of-flight mass spectroscopy (ATOFMS) can provide great detail on the elemental composition of the particles, but only a single particle at a time, and thus it is difficult to obtain representative samples.

This overview of available instruments is not comprehensive. Further details on these methods and others are provided in several reviews, such as that by Witze[5] and references therein. For a review of common optical methods, such as line-of-sight light extinction and light scattering

techniques, refer to Zhao and Ladommatos[8] and references therein. Laser-induced incandescence (LII) is a technique that has recently been applied for quantitative particulate measurements, and is discussed in detail in the remainder of this chapter.

3. CONVENTIONAL LASER-INDUCED INCANDESCENCE (LII) METHOD

3.1 Background

Laser-induced incandescence (LII) is rapidly emerging as a useful diagnostic for acquiring spatially and temporally resolved quantitative measurements of soot particle volume fraction over a very wide range of soot concentrations. Recent comparisons of the method have been made with the gravimetric sampling technique,[9] and there have been some successful measurements of the soot primary particle size.[10] Since the identification of the phenomenon by Eckbreth,[11] laser-induced incandescence (LII) has undergone significant research and development as well as evaluation over a range of conditions and different applications. This method for measuring soot volume fraction and primary particle size produced by combustion systems has the advantages of offering a very wide measurement and dynamic range with a sensitivity estimated to be better than one part per trillion (~2 $\mu g/m^3$). The measurements are made with high spatial and temporal resolution allowing in situ measurements of the time-resolved soot emissions.

Although the theory and analysis associated with the method, which involves nanosecond time response to nanoscale particles, is complex, the application of the method is relatively straightforward. With this technique, a pulsed laser with light pulse duration below 20 nanoseconds is used to rapidly heat the soot particles within the measurement volume from the local ambient temperature to close to the soot sublimation temperature (>4000 K). Incandescence from the soot particles is sensed by a photodetector and the signal is recorded for subsequent analysis. Complex analysis of the nanoscale heat and mass transfer space and time are required in describing the laser light energy absorption by the soot particles and the subsequent cooling process.

LII has a well-defined but complex response to volatile particulate matter. It is insensitive to liquid particles, because they absorb a negligible amount of laser energy compared to carbon. For carbon particles coated with

volatile material, the latter
period. In general, it is r
fraction of carbonaceous r
also be present at low
emissivity relative to carb
resulting in a negligible co

The LII technique is c
vehicle operation, making
diesel engine soot emissi
limited by the repetition
30 Hz, which corresponds
3600 rpm). Therefore, v
resolution in real-time, en
used to reconstruct cycle-r
measurement frequency is
transients, such as those th

LII measurements ge
volume fraction and thus,
signal to the soot concen
results to a system with
methods is used to calibra
is scaling of the LII signal
in a laminar diffusion f
measurements, as shown ir

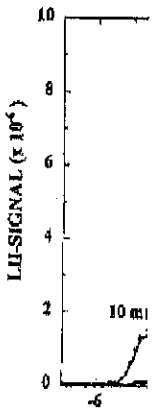

Figure 2. Calibration by compa
extinction (Ni et al.[12]) [–

volatile material, the latter are believed to vaporize early in the laser heating period. In general, it is reasonable to state that LII measures the volume fraction of carbonaceous material in the exhaust. Although metallic ash may also be present at low concentrations, it has a low absorptivity and emissivity relative to carbon and is unlikely to survive the high temperatures, resulting in a negligible contribution to the incandescence.

The LII technique is capable of real-time measurements during transient vehicle operation, making it a valuable tool for optimizing gasoline and diesel engine soot emissions performance. The measurement frequency is limited by the repetition rate of high-power pulsed lasers (typically 10 to 30 Hz, which corresponds to one measurement per engine cycle at 1200 to 3600 rpm). Therefore, while it is not possible to obtain crank-angle resolution in real-time, ensemble-averaging for many engine cycles can be used to reconstruct cycle-resolved transient behavior. However, the real-time measurement frequency is more than adequate to observe engine and vehicle transients, such as those that occur in driving cycles.

LII measurements generally provide a relative measure of the soot volume fraction and thus, a means for calibration is required to relate the signal to the soot concentration. Conventionally, a comparison of the LII results to a system with a soot volume fraction measured by traditional methods is used to calibrate the instrument. One method frequently reported is scaling of the LII signals to match the soot volume fraction (SVF) profile in a laminar diffusion flame as determined by line-of-sight extinction measurements, as shown in figure 2.

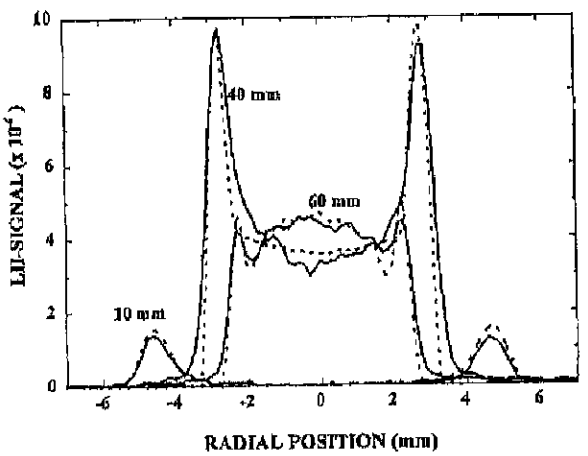

Figure 2. Calibration by comparison of the LII signal to the SVF profiles obtained by laser extinction (Ni et al.[12]) [——— LII data; - - - - laser extinction/scattering data]

In addition to measuring soot concentration, the LII signal can also be interpreted to determine the active surface area of the particle, which in turn can be used to resolve the primary particle diameter. LII has also been used in a semi-quantitative sense to visualize two-dimensional soot distributions for applications in flames, in-cylinder engine measurements, microgravity experiments, etc. An extension of the two-dimensional measurements has been demonstrated, as shown in figure 3, by recording multiple parallel equidistant planes simultaneously, and performing tomographic analysis to reconstruct a three-dimensional image of soot distribution.

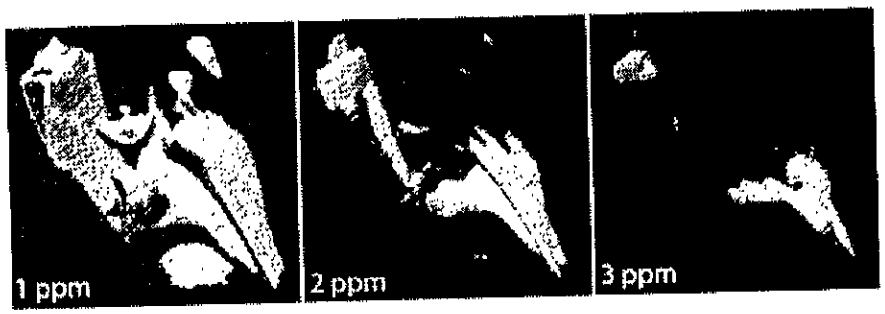

Figure 3. 3-D iso-concentration surfaces acquired in a turbulent non-premixed flame representing soot volume fractions of 1, 2, and 3 ppm, respectively[13]

In the following sections, the state-of-the-art model describing nanoscale (time and space) heat transfer to and from the soot particles will be presented, the approach used for measuring soot volume fraction and primary particle size will be discussed, and representative experimental results showing the recently developed capabilities will be presented and discussed. For a further review of prior LII theory, experimental approaches and practical applications, reference material is available.[14]

3.2 Theory

3.2.1 Heat Transfer Model

The first effort to model the nanoscale heat and mass transfer processes of soot in LII was made by Eckbreth.[11] Subsequent improvement and application of this model have been presented by Melton,[15] Dasch,[16] Tait and Greenhalgh,[17] Hofeldt,[18] and recently by Mewes and Seitzman,[19] Snelling et al.,[20] McManus et al.,[21] Will et al.,[22,23] Snelling et al.,[23] and Schraml et al.[24] An adequate treatment of the sublimation term is the key to the success of a conventional LII model to predict the time-resolved soot particle size, soot

temperature, and the exci
particle size and provides
further rise of soot particle

Soot absorbs and emit
particles. The laser light
size, and the emitted inca
following assumptions app

a) soot primary particle
(Rayleigh regime)
b) laser heating increas
regardless of size
c) when the particles re
absorbed energy goe
that the particles ren
the laser heating per
d) sublimation causes r
incandescent radiati
fluence above the su

The analysis outlined
improved upon the analy
described as aggregates
suggested by Dobbins an
transfer model only consi
equation for the energy b
heating (by a ~10 ns laser

$$C_a q = \frac{2k_a(T - T_k)\pi}{(d_p + G\lambda_f)}$$

The first term represe
aggregate where q is a fu
C_a is the soot absorption c
where ρ_p is the soot densit
particles.

In this analysis, the so
touching primary spheres
within the Rayleigh limit.
soot is expressed as follow

temperature, and the excitation curve. Soot sublimation reduces the soot particle size and provides an effective cooling mechanism that limits the further rise of soot particle temperature.

Soot absorbs and emits light predominantly on the scale of the primary particles. The laser light heating process in LII is independent of particle size, and the emitted incandescent light is nominally volumetric, when the following assumptions apply:

a) soot primary particles are small compared to the laser wavelength (Rayleigh regime)
b) laser heating increases the temperature of all particles at the same rate, regardless of size
c) when the particles reach the sublimation temperature, additional absorbed energy goes into sublimation rather than sensible energy, so that the particles remain at the same temperature for the duration of the laser heating period and
d) sublimation causes negligible particle-size reduction, so that the incandescent radiation from the particles is independent of laser fluence above the sublimation threshold.

The analysis outlined follows the work of Snelling, et al.[20,23] who improved upon the analyses of Hofeldt.[18] Soot particles are frequently described as aggregates of N_p soot primary particles of diameter d_p, as suggested by Dobbins and Megaridis,[25] that are just touching. The heat transfer model only considers isolated primary particles. The heat transfer equation for the energy balance for a soot particle experiencing transient heating (by a ~10 ns laser light pulse) is given as

$$C_a q - \frac{2k_a(T-T_g)\pi d_p^3}{(d_p + G\lambda_f)} + \frac{\Delta H_v(T)}{M_v(T)}\frac{dM}{dt} + q_{rad} - \frac{\pi d_p^3}{6}\rho_p c_p \frac{dT}{dt} = 0 \qquad (1)$$

The first term represents the absorbed laser light energy by the soot aggregate where q is a function describing the laser intensity in W/cm^2 and C_a is the soot absorption cross section. The last term is the laser light heating where ρ_p is the soot density (g/cm^3) and c_p is the specific heat of the carbon particles.

In this analysis, the soot aggregates are taken as an agglomerate of just touching primary spheres of nearly monodisperse diameter d_p that are well within the Rayleigh limit. Furthermore, the absorption coefficient C_a for the soot is expressed as follows

$$C_a = \frac{\pi^2 d_p^3 E(m)}{\lambda} \tag{2}$$

For a wavelength of 1064 nm and a refractive index obtained from the dispersion relationship from Dalzell and Sarofim,[26] $m = 1.63 + 0.7i$ and $E(m) = 0.30$ while at 532 nm, $m = 1.59 + 0.58i$ and $E(m) = 0.26$.

The second term in equation (1) describes the heat transfer to the surrounding medium, where T_g is the ambient gas temperature and T is the instantaneous particle temperature. In the expression, G is a geometry dependent heat transfer coefficient specified as

$$G = \frac{8f}{\alpha(\gamma+1)} \tag{3}$$

where f is the Eucken factor equal to 5/2 for monatomic species, α is the accommodation coefficient now assumed to be ~0.26, $\gamma = c_p/c_v$ (= 1.4 for air) is the ratio of specific heat coefficients. Snelling et al.[20] reported the work of Leroy et al.[27] in which they made measurements indicating that the accommodation coefficient of nitrogen on solid graphite in the temperature range of 300 to 1,000 K gave a value of 0.26.

This second term in equation (1) considers the case of the transition regime between free molecules and a continuum. In laboratory flame environments the soot aggregates are generally smaller than the molecular mean free path length, λ_f. That is, the Knudsen number, $K_n = \lambda_f/d_p$ is much greater than 1 and hence, the heat transfer coefficient is independent of the particle size. It should also be noted that in the denominator, $G\lambda_f >> d_p$ so the dependence of the soot particle diameter becomes insignificant in this term. In other environments such as engine exhaust, the mean free path is significantly shorter, and the Knudsen number is closer to 1.

The third term in equation (1) describes the loss of heat from the particle due to sublimation of the carbon, where $\Delta H_v(T)$ and $M_v(T)$ are the particle temperature dependent heat of evaporation of soot and soot vapor molecular weight, respectively, M is the mass of soot particle, and t is time. The rate of mass loss is given by the analysis of Hofeldt[18] assuming that the particle surface is essentially stationary and that the vapor is lost by diffusion is given as

$$\frac{dM}{dt} = \frac{\rho_p}{2}\pi d_p^2 \frac{dd_p}{dt} = -\frac{\pi d_p^2 N_v M_v}{N_{Av}} \tag{4}$$

where N_v is the molecul
condition (K_n>>1) and N_{Av}

The fourth term in eq
primary particle given as

$$q_{rad}$$

where σ_{SB} is the Stefan-B
is evaluated at the wavele
heat loss due to radiation i

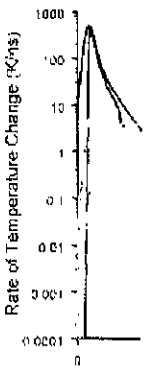

Figure 4. Model results illust
terms on th

Identification of errors
development of this state-
space) heat transfer to
understanding of the phy
This model has been enh
the time-resolved behavic
Figure 4 shows the variot
time.

3.2.2 Excitation Cur

The relationship betw
referred to as the excita

where N_v is the molecular flux of carbon vapor for the free molecular condition (K_n>>1) and N_{AV} is Avogadro's number.

The fourth term in equation (1) describes the radiative heat loss by a primary particle given as

$$q_{rad} = 4\pi^2 \sigma_{SB} T^4 \left(\frac{E(m)}{\lambda} \right) \quad (5)$$

where σ_{SB} is the Stefan-Boltzman constant and the parenthetical expression is evaluated at the wavelength of interest. Compared to the other terms, the heat loss due to radiation is insignificant.

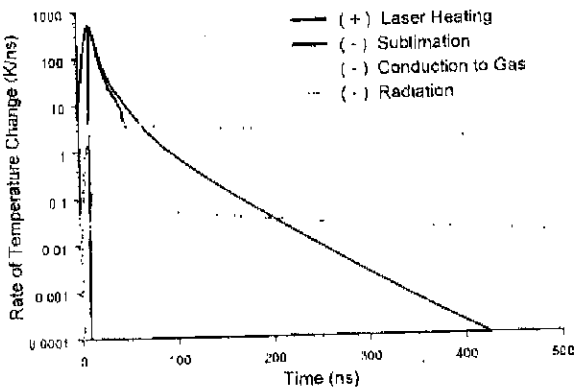

Figure 4. Model results illustrating the time dependent effect of the various heat transfer terms on the rate of temperature change of the particle

Identification of errors propagated through the literature has led to further development of this state-of-the-art numerical model of nanoscale (time and space) heat transfer to and from the particles, in order to support understanding of the physical processes occurring during the LII event.[28] This model has been enhanced to the point where it does well in predicting the time-resolved behavior of the LII signals for a range of laser fluence. Figure 4 shows the various terms of the heat transfer model as a function of time.

3.2.2 Excitation Curve

The relationship between the LII signal and the excitation fluence is referred to as the excitation curve. The spatial distribution of laser light

fluence can have a significant effect upon the measured LII signal level, as shown in the excitation curves presented in figure 5. Regardless of the spatial fluence profile, as the energy of the laser light is increased there is an initial sharp increase in LII signal. A peak laser fluence can be reached such that a further increase in energy produces very little increase in LII signal. Conventional LII is typically operated in this "plateau" region, where the LII signal is somewhat independent of the laser fluence.[12,16,17,20,29,30] The behavior at fluence beyond the plateau region is dramatically different for the "top-hat" profile in comparison to the Gaussian profile. This is due to sublimation of the carbon causing a mass (and volume) loss. For the "top-hat" profile, this results in a decrease in the LII signal. For the Gaussian profile, the decrease in the LII signal due to mass loss at the center of the laser light beam where the peak fluence is located is offset by the increasing contribution from the "wings" of the spatial profile, resulting in a slight increase in the overall LII signal.

The variation in the spatial profile for a Gaussian light beam means that the particles in the probe volume will be heated to different temperatures, making theoretical interpretation of the LII signals much more difficult.

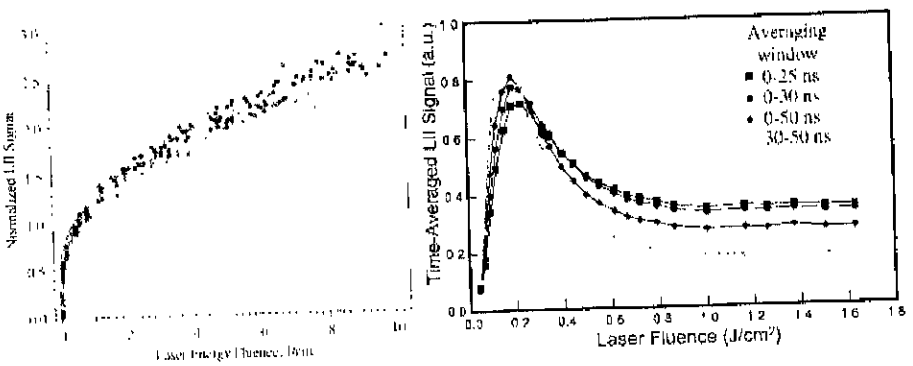

Figure 5. Fluence dependence of LII signal as a function of laser beam spatial profile: left, Gaussian profile (Shaddix and Smyth[30]) and right, "top-hat" profile (Witze et al.[31])

3.2.3 Soot Volume Fraction (SVF)

In order to determine the soot volume fraction, the LII signal must be scaled to data obtained in a source of known volume concentration. Frequently, the source has been a laminar flame which has been characterized by line-of sight extinction.

To obtain radially-resolved spatial information, the three-point Abel algorithm of Dasch[32] can be applied to invert the line-of-sight transmission

measurements. Details of a
by Snelling et al.[33] For visib
concentration are expected
soot aggregates. There are
soot and its wavelength dep

LII measurements can b
flame and then scaled by a
in figure 2, so that the inte
width is as close as possibl
general it has been observe
profiles from LII and Abe
range from 0.5 to 5 ppm.[
for calibration, has observ
concentration range.[35]

3.2.4 Primary particle

Immediately after the l
the particles is conduction
primary particles, the temp
the ambient gas, T_g, decay
period. An equation of the f

is fit to the temperature
exponential decay, where
knowledge of the ambient
thermocouple. The primar
from the decay of the LII
fitting the decay of temp
(e.g. as in Schraml et al.[3
known to have shortcoming

ed LII signal level, as
5. Regardless of the
is increased there is an
ce can be reached such
increase in LII signal.
" region, where the LII
ience.[12,16,17,20,29,30] The
matically different for
profile. This is due to
ne) loss. For the "top-
gnal. For the Gaussian
oss at the center of the
offset by the increasing
e, resulting in a slight

light beam means that
different temperatures,
ich more difficult.

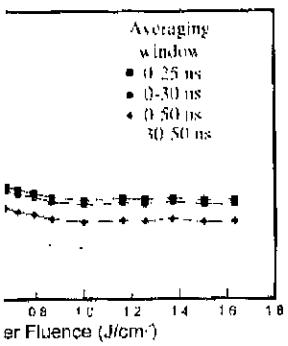

aser beam spatial profile:
at" profile (Witze et al.[31])

. the LII signal must be
volume concentration.
lame which has been

n, the three-point Abel
ine-of-sight transmission

measurements. Details of an enhanced two-dimensional technique are given by Snelling et al.[33] For visible wavelengths, errors of 30% and greater in soot concentration are expected depending on the size and morphology of the soot aggregates. There are significant uncertainties in the refractive index of soot and its wavelength dependence which can mask such effects.[20]

LII measurements can be performed at the same locations in the laminar flame and then scaled by a single factor to the Abel-inverted data as shown in figure 2, so that the integrated soot volume fraction over the total flame width is as close as possible for the extinction and LII data at all heights. In general it has been observed that there is linear agreement between the soot profiles from LII and Abel inverted transmission measurements over the range from 0.5 to 5 ppm.[12,20,29,34] Vander Wal, using gravimetric sampling for calibration, has observed good linearity in the 0.035 to 1.5 ppm soot concentration range.[35]

3.2.4 Primary particle diameter

Immediately after the laser pulse, the dominant cooling mechanism for the particles is conduction to the surrounding gas. Assuming monodisperse primary particles, the temperature difference between the particles, T, and the ambient gas, T_g, decays steadily in an exponential manner during this period. An equation of the form

$$T - T_g = A \cdot e^{-t/\tau} \tag{6}$$

is fit to the temperature data to determine τ, the time constant of the exponential decay, where A is a constant. This method requires *a priori* knowledge of the ambient gas temperature, which may be determined by thermocouple. The primary particle diameter can be determined directly from the decay of the LII signal, as shown in figure 6. The advantage in fitting the decay of temperature rather than the decay of the LII signal (e.g. as in Schraml et al.[36-38]) is that the heat transfer models which are known to have shortcomings[28] do not need to be relied upon.

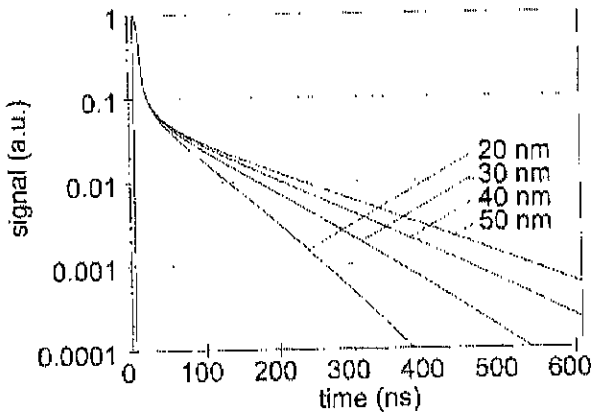

Figure 6. Numerically modeled LII signal decay of soot at STP ambient conditions for a range of primary particle diameters, normalized to the maximum (Schraml et al.[37])

The particle diameter d_p is then determined from the relation derived from McCoy and Cha[39]

$$d_p = \frac{12 k_g \alpha \tau}{G \lambda_l c_p \rho_p} \tag{7}$$

where k_g is the thermal conductivity of the ambient gas, α is the thermal accommodation coefficient, G is a geometry-dependent heat transfer coefficient, and c_p is the specific heat of the particle.

3.3 Issues With Conventional LII

Although the LII process is essentially nonintrusive, it is not completely non-perturbing as the laser light heating can be expected to affect the soot morphology[40] and cause some sublimation during the short pulse of laser light. It is anticipated that the particulates undergo optical and physical property changes as a function of time, fluence, and their composition. The particles may become more structured (graphitized), and may become hollow shells as the sublimation occurs from the core outwards.

For particle sizing, the p
which cannot be determine
there is uncertainty in the v
to the significant sublimat
than before the measurem
carbon vapor (Stephan flov
and affect the heat conduct
cooling rate of the particle
particle temperatures after
make it very difficult to m
cooling of the particle, as it
as a function of tempe
monodisperse primary par
combustion systems.

For determining the sc
between the calibration a
volume concentration shou
created equal. Calibrating i
at lower temperatures ca
temperatures. Furthermore
an effect, as it impacts
carbon. Even calibration
composition of the particu
again resulting in different
will also affect the sensiti
parameters.

In dense particulate fie
lengths, there will be issu
trapping of the LII signal
dimensional laminar flows
practical environments wi
correction could be applied

4. SELF CALIB

4.1 Innovations

The standard practice f
the LII systems in a ste

TP ambient conditions for a
ximum (Schraml et al.[37])

rom the relation derived

(7)

nt gas, α is the thermal
lependent heat transfer

sive, it is not completely
pected to affect the soot
the short pulse of laser
go optical and physical
d their composition. The
zed), and may become
e outwards.

For particle sizing, the parameter of greatest interest is the aggregate size, which cannot be determined by LII. In determining the primary particle size, there is uncertainty in the value of the accommodation coefficient. Also, due to the significant sublimation which occurs, the particles may be smaller than before the measurement, and they are surrounded by a cloud of hot carbon vapor (Stephan flow), which will reduce the diffusion to the particle and affect the heat conduction to the surrounding medium and therefore the cooling rate of the particles. This is what causes the higher than expected particle temperatures after a high fluence laser light pulse.[24] These issues make it very difficult to model the physics of the transient sublimation and cooling of the particle, as it is unclear what the appropriate gas properties are as a function of temperature and time. Finally, the assumption of monodisperse primary particles is unlikely to hold true for most practical combustion systems.

For determining the soot volume fraction, as long as nothing changes between the calibration and the LII measurements of particulates, the volume concentration should be accurate. However, all particulates are not created equal. Calibrating in a flame at high temperature and then measuring at lower temperatures can introduce inaccuracies due to different peak temperatures. Furthermore, variation in the ambient pressure can also have an effect, as it impacts upon the sublimation temperature of elemental carbon. Even calibration in engine exhaust will result in errors, as the composition of the particulates can change as the engine conditions change, again resulting in different peak temperatures. The spatial light beam profile will also affect the sensitivity of the LII signal to these variations in other parameters.

In dense particulate fields, or those with exceptionally long optical path lengths, there will be issues with attenuation of the laser light beam and trapping of the LII signal generated in the probe volume. In simple two-dimensional laminar flows these effects may be corrected for. However, in practical environments with turbulent flows, it is unlikely that an accurate correction could be applied.

4. SELF CALIBRATING LII (SC-LII) METHOD

4.1 Innovations

The standard practice for measuring soot volume fractions is to calibrate the LII systems in a steady-state flame using extinction measurements.

Recently, however, a novel technique for performing absolute light intensity measurements in LII has been presented, thus avoiding the need for a calibration in a source of soot particulates with a known concentration,[41,42] and thus extending the capabilities of LII for making practical quantitative measurements of soot. The use of the absolute intensity approach provides for continuous *in situ* self-calibration of the LII technique, and allows use of lower laser fluence and lower maximum soot temperatures. This low fluence approach simplifies interpretation of the data and eliminates most of the uncertainties, with the exception of the optical properties. Thus, issues associated with sublimation of a significant portion of the soot are avoided. The absolute intensity method is a time-resolved approach that applies two-color pyrometry principles to determine the particle temperatures, relating the measured signals to the absolute sensitivity of the system as determined with a traceable source. The time-resolution and temperature data are important for understanding the LII process and improving the associated nonequilibrium heat and mass transfer model.

4.1.1 Self Calibration

The spectral sensitivity of the detection system is determined by calibrating with an extended source of known radiance, such as a strip filament lamp.[41] This sensitivity is then used to interpret the measured LII signals, which provides the required soot particle temperature, and results in absolute intensities ($W/m^3 \cdot sr$). This method offers advantages in that it is:

a) NIST-traceable
b) not susceptible to: fluctuations in laser fluence; laser beam attenuation by the soot; or condensed volatiles on the particles and
c) knowledge of the ambient temperature is not needed to determine soot concentration.

4.1.2 Two-Color Pyrometry

Two-color pyrometry is applied to measure primary particle temperature history, which can be used with the absolute intensities of the LII signal to determine time-resolved soot volume fraction,[42] as shown in figure 7. Note that there is no evidence of the rapid drop in LII signals common with sublimation, and that peak temperatures are less than 4000 K. More information about pyrometry is available in Chapter 10.

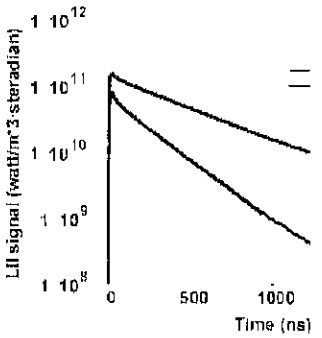

Figure 7. Absolute LII signal int
the transien

4.1.3 Laser Beam Pro

As the intensity of LII
accurate measurements der
volume. To achieve this, a
techniques can be employe
the probe volume:

a) expand the beam inte
collection, and use ar
view to the central pc
probe volume size, ar
b) use a vertical-slit ape
in the depth-of-field
slit plane to the probe

The resulting near-top-hat s

4.1.4 Low Laser Fluer

Conventional LII is per
assure that the particles are
the sublimation of carbon
"independent" of the laser f
to be measured.

Typically, a laser light
used, based on the assu
insignificant. However, as
can be significant. With the

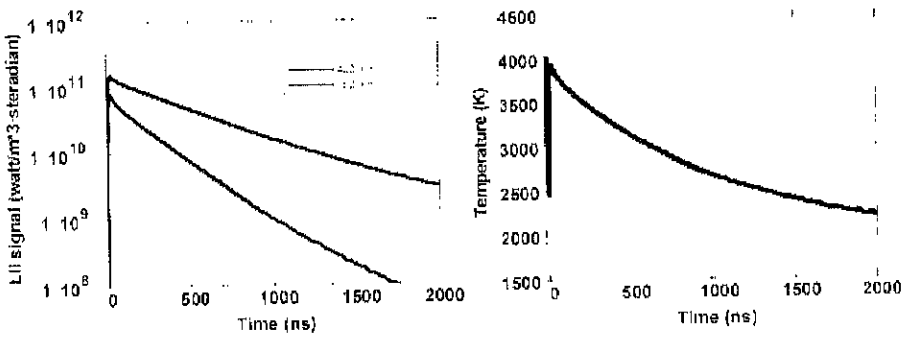

Figure 7. Absolute LII signal intensities and the resulting determination of temperature during the transient heating and cooling of soot particles[42]

4.1.3 Laser Beam Profile

As the intensity of LII signals depends upon the particle temperature, accurate measurements demand uniform heating of all particles in the probe volume. To achieve this, a true top-hat laser spatial profile is required. Two techniques can be employed to optimize the uniformity of the laser beam at the probe volume:

a) expand the beam into a sheet in the plane normal to the axis of signal collection, and use an iris in the detection optics to restrict the field-of-view to the central portion of the beam (the iris allows us to vary the probe volume size, and thus signal intensity), and
b) use a vertical-slit aperture to pass just the central portion of the beam in the depth-of-field direction of the receiver lens, and relay image the slit plane to the probe volume.

The resulting near-top-hat spatial profile is shown in figure 8.[43]

4.1.4 Low Laser Fluence

Conventional LII is performed using laser light fluence high enough to assure that the particles are heated to temperatures greater than required for the sublimation of carbon (~4000 K). This is done so that the LII signal is "independent" of the laser fluence. Hence particle temperature does not need to be measured.

Typically, a laser light fluence considerably greater than 0.2 J/cm^2 is used, based on the assumption that mass loss from sublimation is insignificant. However, as shown in figure 9, mass loss from laser heating can be significant. With the low-fluence LII technique, the particles are kept

below the sublimation temperature. Quantitative low fluence LII can only be performed in conjunction with the absolute intensity calibration, as the absolute intensity method provides a direct measure of the particle temperature.

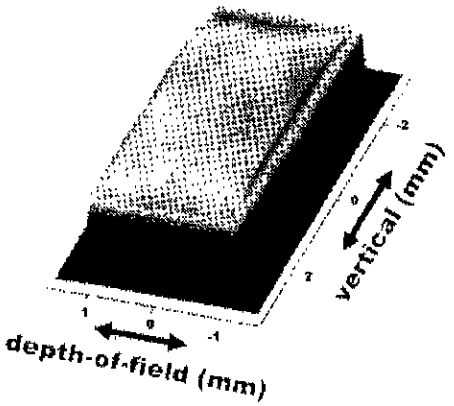

Figure 8. Measurement of the optimized laser beam profile at the LII probe volume demonstrating uniformity of fluence.[43] The central 2 mm (vertical) is imaged onto the detectors.

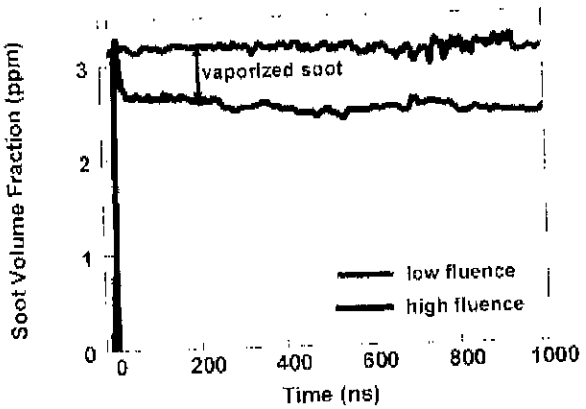

Figure 9. Real-time measurements of soot volume fraction showing no sublimation at low fluence and ~20% volume change at a higher fluence, occurring within 50 ns of the beginning of the laser pulse

4.2 Theory

Self-calibrating LII (SC
surface temperature. dete
independent wavelengths
temperature across the lase
observed signals (correcte
particle absorption cross s
source of known radiance,
the measured signals to t
W/m^3·sr)

where $V_{coll}(\lambda)$ is the obser
the spectral radiance of th
collection efficiency of t
detection wavelength λ.

The power radiated by
is given by[41, 42]

$$P_p(\lambda) =$$

where h and k are Planck
velocity of light. The spe
power radiated by a single
probe volume, $N_{PV} = n_p($
primary particles in the
represents the volume int
laser light sheet and A_p i
viewed by the detection sy
must be measured experi
calibration and the particl
the particles in the probe v

4.2 Theory

Self-calibrating LII (SC-LII) is based upon knowledge of the particulate surface temperature, determined by optical pyrometry. If two or more independent wavelengths λ are recorded, an average soot particle surface temperature across the laser sheet can be calculated by using the ratio of the observed signals (corrected for detection sensitivity) and the known soot particle absorption cross sections. A single point calibration is made with a source of known radiance, which provides calibration factors η(λ) to relate the measured signals to the absolute spectral intensities of the source (in $W/m^3 \cdot sr$)

$$\eta(\lambda) = \frac{V_{CAL}(\lambda)}{R_S(\lambda, T)} \tag{8}$$

where $V_{CAL}(\lambda)$ is the observed signal from the calibration lamp and $R_S(\lambda,T)$ is the spectral radiance of the lamp. The calibration factor η accounts for the collection efficiency of the receiver and the detector responsivity at the detection wavelength λ.

The power radiated by a single particle of diameter d_p into 4π steradians is given by[41, 42]

$$P_p(\lambda) = \frac{8\pi^3 c^2 h}{\lambda^6}\left(e^{\frac{hc}{k\lambda T}} - 1\right)^{-1} d_p^3 E(m_\lambda) \tag{9}$$

where h and k are Planck and Boltzmann constants, respectively, and c is the velocity of light. The spectral radiance of the soot is dependent upon the power radiated by a single particle $P_p(\lambda,T)$ and the number of particles in the probe volume, $N_{PV} = n_p(w_b A_p)$, where n_p represents the concentration of primary particles in the probe volume, and the quantity in parentheses represents the volume interrogated, with w_b as the equivalent width of the laser light sheet and A_p is the cross-sectional area of the probe volume as viewed by the detection system. The equivalent width of the laser light sheet must be measured experimentally. Since this area is the same for both the calibration and the particle measurement, an equivalent spectral radiance for the particles in the probe volume R_p can be defined as

$$R_p(\lambda) = \frac{P_p(\lambda) n_p w_b}{4\pi} \tag{10}$$

which can be related to the observed signal from the particles $V_{EXP}(\lambda)$ by the calibration factor $\eta(\lambda)$, such that

$$\eta = \frac{4\pi \cdot V_{EXP}(\lambda)}{P_p(\lambda) n_p w_b} \tag{11}$$

The observed signal ratio at the two wavelengths $V_{EXP}(\lambda_1)/V_{EXP}(\lambda_2)$ can be converted to relative particle radiance using the calibration factors

$$\frac{P_p(\lambda_1)}{P_p(\lambda_2)} = \frac{V_{EXP}(\lambda_1)}{V_{EXP}(\lambda_2)} \frac{\eta(\lambda_2)}{\eta(\lambda_1)} \tag{12}$$

The ratio of the powers at two wavelengths radiated by a single particle is given by

$$\frac{P_p(\lambda_1)}{P_p(\lambda_2)} = \frac{\lambda_2^6}{\lambda_1^6} \frac{\left(e^{\frac{hc}{k\lambda_2 T}} - 1\right)}{\left(e^{\frac{hc}{k\lambda_1 T}} - 1\right)} \frac{E(m_{\lambda_1})}{E(m_{\lambda_2})} \tag{13}$$

Using the experimentally determined power ratio from equation (12), the known values of $E(m_\lambda)$, and assuming all the particles in the probe volume are heated to the same temperature, equation (13) can be solved for T. It is the relative, not the absolute, magnitude of the particle absorption function at the two wavelengths that is important in determining soot particle surface temperature. For the work presented here, the values for $E(m_\lambda)$ were those determined by Krishnan et al.[44]

The particle (soot) volume fraction is given by

$$f_v = n_p \cdot \frac{\pi d_p^3}{6} \tag{14}$$

Expressing equation (9) in terms of d_p^3, and equation (11) in terms of n_p, and substituting into equation (14), the soot volume fraction is then

$$f_v = \frac{V_{EXP}(\lambda)}{\eta(\lambda) w_b} \frac{\lambda^6 \left(e^{\frac{hc}{k\lambda T}} - 1\right)}{12\pi c^2 h\, E(m_\lambda)} \tag{15}$$

The soot volume fraction has an inverse dependence on the absolute magnitude of the particle absorption function.

4.3 Limitations a

Differences between tl
SC-LII and the total PM m
several factors. These fac
fraction to the relevant pro
uncertainties in the SC-LI
by the other techniques.

The uncertainties in th
due to uncertainty in the
particular, one must know
to correctly determine the
determine the concentratic
relative value of $E(m_\lambda)$ at
data of Krishnan et al.[44]
400 to 800 nm. However,
over the visible to near-in
Sensitivity analysis indica
this magnitude will result
order of 50%. Similarly,
indicates a 1:1 correspond
of $E(m_\lambda)$ leads to a
Furthermore, $E(m_\lambda)$ may
altered as it is heated by
also affect the soot absorp

A minor uncertainty
manner is in the knowle
detection system for each
source changes, whethe
particles, the effective c
dichroic mirror, interfe
nonlinear yet predictable
short wavelengths, low
monotonically with incr
could be corrected for wi

In order to compare
particulates is required to
average density for dry
wide range in the densit
(2.26 g/cm^3).

As the primary part
proportional to the sur

4.3 Limitations and Sources of Error

Differences between the volume concentration of soot measured with SC-LII and the total PM measured with other techniques can be attributed to several factors. These factors include: uncertainty in relating soot volume fraction to the relevant property of the PM measured by the other techniques; uncertainties in the SC-LII technique; and uncertainty and errors introduced by the other techniques.

The uncertainties in the absolute intensity approach to LII are primarily due to uncertainty in the soot refractive index at elevated temperatures. In particular, one must know the relative value of $E(m_\lambda)$ at the two wavelengths to correctly determine the temperature, and the absolute value of $E(m_\lambda)$ to determine the concentration once the temperature has been determined. The relative value of $E(m_\lambda)$ at the two wavelengths based on the best available data of Krishnan et al.[44] increases ~20% with wavelength over the range 400 to 800 nm. However, recent results from Snelling et al.[45] indicate that over the visible to near-infrared range the relative value of $E(m_\lambda)$ is constant. Sensitivity analysis indicates that a change in the relative value of $E(m_\lambda)$ of this magnitude will result in an increase in the soot volume fraction of the order of 50%. Similarly, sensitivity analysis on the absolute value of $E(m_\lambda)$ indicates a 1:1 correspondence, such that a 20% uncertainty in the magnitude of $E(m_\lambda)$ leads to a 20% uncertainty in the soot volume fraction. Furthermore, $E(m_\lambda)$ may vary with temperature as the soot structure may be altered as it is heated by LII, and if present, condensed organic species may also affect the soot absorption function.

A minor uncertainty which also affects the accuracy in a systematic manner is in the knowledge of the effective center wavelength of the light detection system for each of the two wavelengths. As the temperature of the source changes, whether it is the calibration lamp or the heated soot particles, the effective center light wavelength of the combination of the dichroic mirror, interference filter, and detector response varies in a nonlinear yet predictable manner. This systematic inaccuracy is greatest for short wavelengths, low temperatures, and large bandwidths, reducing monotonically with increasing temperature. The error is less than 5%, and could be corrected for with an iterative approach to the data analysis.

In order to compare with mass concentration, the bulk density of the particulates is required to convert the volume fraction measured with LII. An average density for dry soot (1.9 g/cm^3) is often used, although there is a wide range in the densities reported in the literature, up to that for graphite (2.26 g/cm^3).

As the primary particle diameter determined from the cooling rate is proportional to the surface area per unit volume (specific surface area)

available for conduction, it is an "effective" or "apparent" size. In addition, the current SC-LII approach treats the particles as individual monosized primary particles, without accounting for the effects of size distribution and aggregation. Due to shielding (dense clusters) and bridging (greater than point contact) of particles in an aggregate, the available specific surface area is substantially reduced, resulting in an apparent primary particle size that is significantly larger than the size one would measure with techniques such as transmission electron microscopy (TEM). Also, the size distributions of both primary particles and aggregates will have an impact upon the primary particle size measurements, as current models assume monodisperse individual primary particles.

Another significant uncertainty is the thermal accommodation coefficient α, which is often ignored (i.e., assigned a value of 1) or assigned a textbook value of 0.9, which may be suitable for equilibrium conditions at room temperature. The thermal accommodation coefficient is the efficiency of heat transfer between gas molecules and a condensed body when gas-surface collisions occur in the free-molecular regime. The value of 0.26 determined by Leroy et al.[27] for carbon under nonequilibrium conditions at elevated temperatures is the current preferred value. However, it is unknown whether this value is valid for the full range of temperatures encountered. This uncertainty may affect the accuracy of the primary particle sizing, but neither the precision, nor the relative comparison of the primary particle sizes obtained for different engine conditions.

As uncertainties in $E(m)$, accommodation coefficient, and particle density only affect the analysis of SC-LII data (and do not require changes to the experimental configuration), previously obtained results can easily be updated as new information becomes available for these quantities.[46]

4.4 Implementation of SC-LII

A fully-integrated, portable system has been developed for soot particulate characterization in various applications, utilizing the key innovations of SC-LII. A schematic layout of the system is presented in figure 10. This system consists of a pulsed Nd:YAG laser, operating with 60 mJ/pulse at 20 Hz and 1064 nm. A half-wave plate (to rotate the plane of polarization) in combination with a thin film polarizer (angle-tuned to transmit horizontally polarized radiation) is used to adjust the laser energy as required. A second half-wave plate is used to return the plane of polarization to vertical. True top-hat profiles are used for all measurements to deliberately ensure that the soot particles are heated to a uniform temperature throughout the sample volume. As a result, there is no direct need to apply

the numerical model descri
fluence LII, ~0.1 J/cm^2, is
≤4000 K, ensuring that neg
is used to measure the
automatically adjusted to m

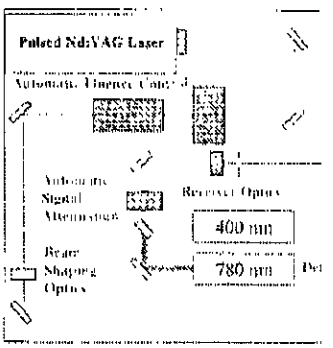

Figure 10. Schemati

The LII signal from th
aperture, which is coupled
unit. The collected LII sign
by two photomultipliers,
centered at 400 and 780 n
system is incorporated to
transient signals from the p
acquisition board and subs
analysis.

4.5 Applications

In addition to the applic
gasoline, and gas turbine en
find application for measure

a) ambient atmospheric
b) soot in pool fires, furn
c) metal and metal oxide
d) material synthesis

The range of volume
demonstrated in a variety of

the numerical model described earlier in the analysis of LII signals. Low fluence LII, ~0.1 J/cm^2, is employed to limit the peak soot temperatures to ≤4000 K, ensuring that negligible soot sublimation occurs. A photodetector is used to measure the transmitted laser energy and the polarizer is automatically adjusted to maintain the desired fluence from pulse-to-pulse.

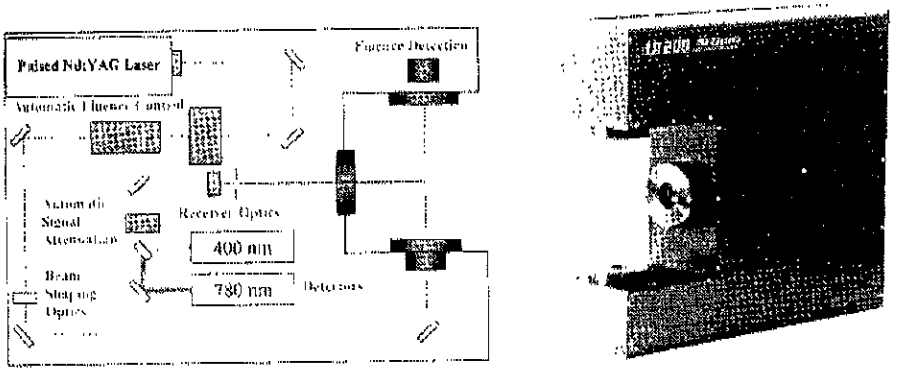

Figure 10. Schematic layout and photograph of an SC-LII system.

The LII signal from the center of the laser beam is imaged onto an aperture, which is coupled to a two-channel color separation and detection unit. The collected LII signal is color separated and independently recorded by two photomultipliers, equipped with narrowband interference filters centered at 400 and 780 nm, respectively. An automatic light attenuation system is incorporated to provide for wide dynamic range detection. The transient signals from the photomultipliers are recorded by a high speed data acquisition board and subsequently transferred to a computer for further analysis.

4.5 Applications

In addition to the applications described in detail below, namely diesel, gasoline, and gas turbine engines, and carbon black production, SC-LII may find application for measurements of:

a) ambient atmospheric elemental carbon concentration
b) soot in pool fires, furnaces, and boilers
c) metal and metal oxide nanoparticles, and
d) material synthesis

The range of volume concentration measurements that have been demonstrated in a variety of applications is illustrated in figure 11.

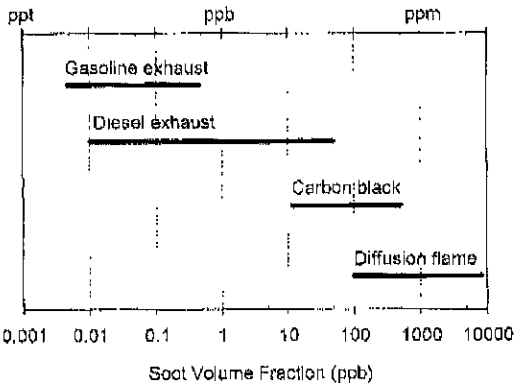

Figure 11. Numerous studies of soot detection illustrate the typical span of concentrations measured for a wide range of applications.

4.5.1 Diesel Engines

Conventional LII has been applied by many to determine the mass concentration of particulates produced by diesel engines.[36,38,47] Figure 12 illustrates the agreement between conventional LII and the AVL filter smoke number (FSN) over a wide range of particulate concentrations.[37] This good agreement is expected, as LII measures the soot concentration, and the FSN is related to the black smoke level, comparable quantities.

Comparison of the particulate concentration data obtained from SC-LII was in good agreement with gravimetric data acquired simultaneously as shown in figure 13. The AVL steady-state simulation of the EPA transient test procedure was used in this example. Under this protocol, engine emissions were measured at steady speed/load conditions. The engine was varied from a low idle speed (600 RPM/0 percent load) to the engine's rated speed and load (1800 RPM/100 percent load).

A weighting scheme was designed to produce composite brake specific emissions to accurately predict the gaseous omissions obtained using the EPA transient test procedure. Since steady-state simulation does not accurately simulate transient engine behavior, these composite PM emissions can only be expected to show the current trends due to engine transients. Some of the discrepancies between the gravimetric and LII results may be attributed to the fact that gravimetric sampling includes an organic fraction that does not contribute to the signal measured by LII and that the density of the particulates is required to convert the mass determined by the gravimetric filter methods to volume fraction for comparison with LII.

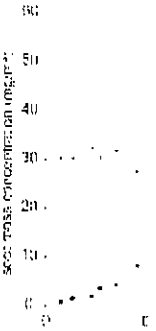

Figure 12. Soot mass concentr
number in the exhaust

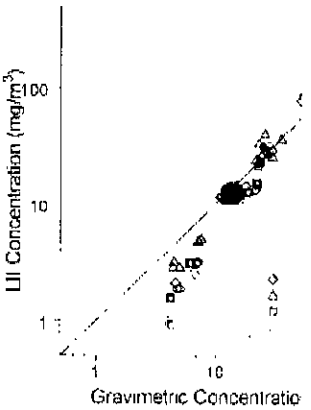

Figure 13. Soot particle conc
concurrently, for four differe
soot concentration measured
AVL stead

Comparisons were also
smoke meter for the eight
shown in figure 13 indi
measurements over 2.5 ord
The solid line in figure 13
dashed line represents perfe
on the graph indicate the
simulation.

rate the typical span of
f applications.

y to determine the mass
engines.[36-38,47] Figure 12
and the AVL filter smoke
oncentrations.[37] This good
oncentration, and the FSN
antities.
lata obtained from SC-LII
cquired simultaneously as
ation of the EPA transient
der this protocol, engine
onditions. The engine was
load) to the engine's rated

e composite brake specific
issions obtained using the
tate simulation does not
or, these composite PM
rrent trends due to engine
gravimetric and LII results
mpling includes an organic
easured by LII and that the
the mass determined by the
comparison with LII.

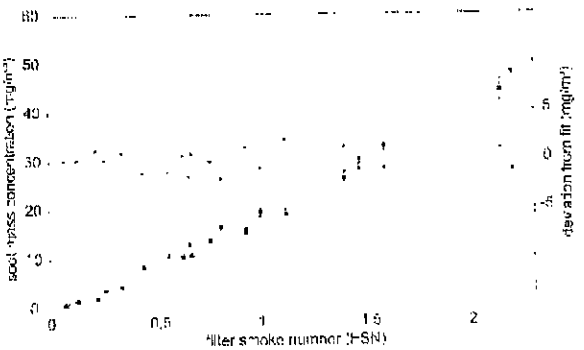

Figure 12. Soot mass concentration from LII measurements as a function of filter smoke number in the exhaust of a medium-duty diesel engine (Schraml et al.[37])

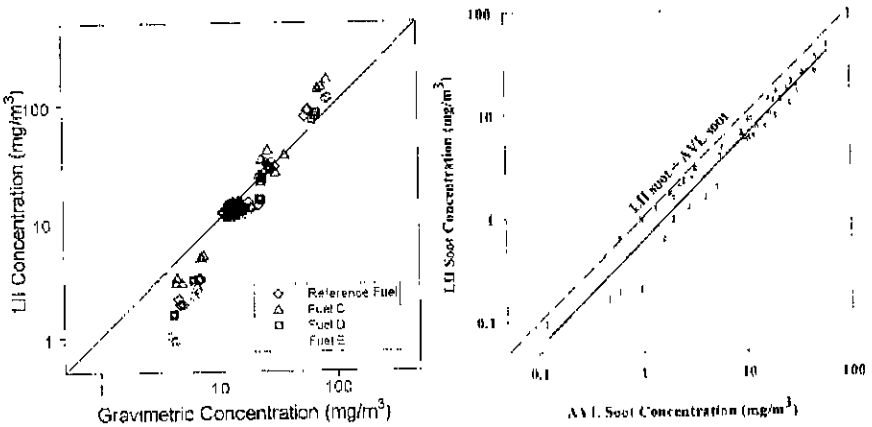

Figure 13. Soot particle concentration determined by the LII and gravimetric methods concurrently, for four different fuels (left; Smallwood et al.[48]) and comparisons of the soot concentration measured with the LII instrument and the AVL smoke meter for the AVL steady-state simulation (right; Neill et al.[49])

Comparisons were also made between the LII instrument and the AVL smoke meter for the eight engine modes in the EPA simulation. The results shown in figure 13 indicates very good correlation between the two measurements over 2.5 orders of magnitude variation in soot concentration. The solid line in figure 13 represents the regression fit to the data and the dashed line represents perfect agreement between the two methods. Numbers on the graph indicate the data points for each mode of the AVL 8-mode simulation.

4.5.2 Gasoline Engines

Data were reported that demonstrate the LII technique's capability for measuring transient emissions, applied to the exhaust from a state-of-the-art production direct injection spark ignition engine.[50] The unmodified engine used a lean burn stratified charge combustion concept for some of its operating modes. Measurements were acquired over a series of transient driving cycles. Concurrent ELPI measurements were acquired for direct comparison. Dilution was unnecessary for the LII method since it responds to only the soot component of the particulates. Any condensed material including the organic fraction of the particulates and water do not contribute to the measured LII signal. The high-energy laser is anticipated to evaporate these volatile materials well before the significant portion of the LII signal is detected.

Measurements using the ELPI instrument were made post dilution so the sampled stream experienced some cooling and consequently, the measured particulates are composed of soot and condensable organic species and trace elements. The ELPI instrument produces measurements at one-second intervals but appears to have a lower temporal response than the LII instrument, as shown in figure 14. In this experiment LII was demonstrated to have sensitivity to concentrations as low as 5 ppt.[50]

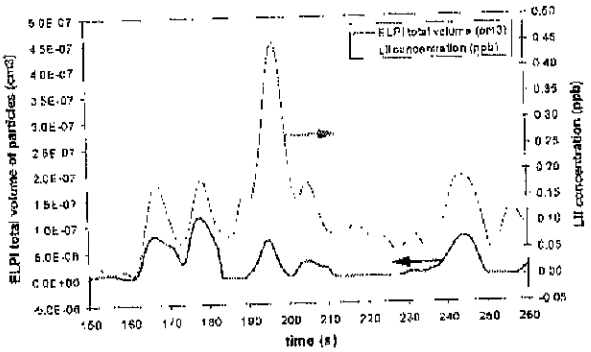

Figure 14. Relative temporal response and sensitivity of LII and ELPI (Smallwood et al.[50])

4.5.3 Gas Turbine Eng

Recently, there has beer measure soot concentration have been reported by Schä have indicated that a measu in diameter in a decided successful demonstrations measurements in a test cell

The spatial and tempora a gas turbine are shown in f in the soot mass concentrati settings. Detailed measure plume will assist designer efficiency, and of signific radiation signature.

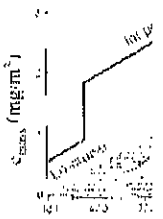

Figure 15. Transverse profi gas turbine engine illu intermediate-to

4.5.4 Carbon Black I

The surface area of a particle size, is a key para only measures the elemen recognized as a potential control application. A cor reactor and analyzed w subsequent analysis with reported.[43]

echnique's capability for
ust from a state-of-the-art
[10] The unmodified engine
concept for some of its
over a series of transient
were acquired for direct
method since it responds
Any condensed material
nd water do not contribute
is anticipated to evaporate
portion of the LII signal is

made post dilution so the
onsequently, the measured
e organic species and trace
surements at one-second
al response than the LII
nent LII was demonstrated
t.[50]

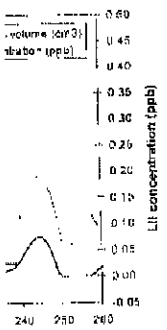

II and ELPI (Smallwood et al.[50])

4.5.3 Gas Turbine Engines

Recently, there has been heightened interest in the application of LII to measure soot concentrations in the exhaust of aviation gas turbines. These have been reported by Schäfer et al.,[51] Allen et al.[52] and Jenkins et al.[53] All have indicated that a measurement across a plume that is of the order of 1 m in diameter in a decidedly hostile environment is difficult. However, successful demonstrations of spatially resolved, real-time, in-situ LII measurements in a test cell environment have been reported.[53]

The spatial and temporal resolution of LII measurements in the plume of a gas turbine are shown in figure 15, which illustrates the significant changes in the soot mass concentration that occur with rapid changes in engine power settings. Detailed measurements of the particulate concentrations in the plume will assist designers in reducing particulate emissions, improving efficiency, and of significance to the military, minimizing the infrared radiation signature.

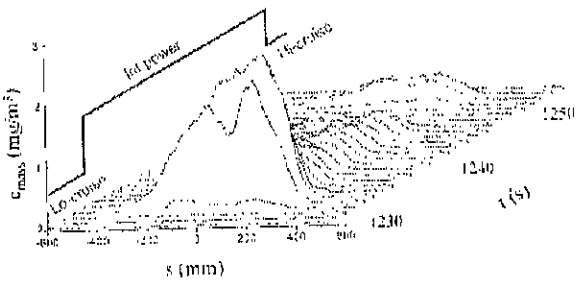

Figure 15. Transverse profiles of soot mass concentration in the exhaust plume of a gas turbine engine illustrating the effect of both low-to-intermediate and intermediate-to-low engine power changes (Jenkins et al.[53])

4.5.4 Carbon Black Reactor

The surface area of aggregated nanoparticles, related to the primary particle size, is a key parameter in the production of carbon black. As LII only measures the elemental carbon portion of the particulates, it has been recognized as a potential method for measuring carbon black in a process control application. A comparison of samples drawn from a carbon black reactor and analyzed with LII to those simultaneously acquired for subsequent analysis with standard laboratory methods has been recently reported.[43]

The carbon black specific surface area, S, can be expressed as

$$S = \frac{\text{surface area}}{\text{mass}} = \frac{\pi \int_0^\infty d^2 p(d_p)\ dd_p}{\rho_p \left(\frac{\pi}{6}\right) \int_0^\infty d^3 p(d_p)\ dd_p} = \frac{6}{\rho_p D_{32}} \tag{16}$$

where D_{32} is the Sauter Mean Diameter (SMD) and $p(d_p)$ is a probability distribution function. As the size determined by LII is proportional to the surface area per unit volume, it should be related to D_{32} as

$$S_{LII} = \frac{6000}{1.8\, d_{p,II}} \tag{17}$$

where $d_{p,II}$ is the apparent primary particle diameter, 1.8 g/cm^3 is a typical density for carbon black particles, and S_{LII} is expressed in m^2/g. LII specific surface area distributions were measured for two carbon black reactor conditions, and were normalized by setting them equal to the independently measured statistical thickness surface area (STSA) value at 100.

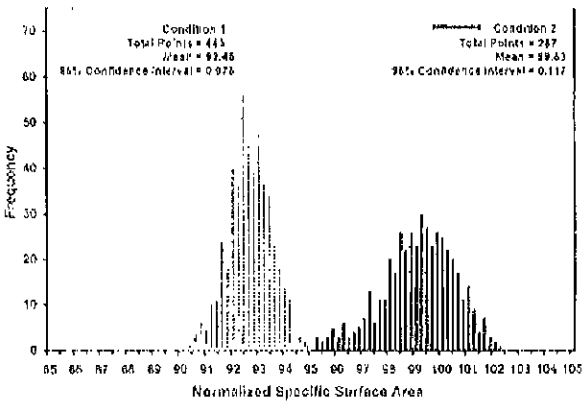

Figure 16. NSSA distributions for two different carbon black reactor conditions[43]

These normalized specific surface area distributions (NSSA) are shown in figure 16, where it can be seen that the 95% confidence intervals on the mean of the NSSA is approximately 0.1%. The width of the distributions of NSSA, as measured by a single standard deviation, is approximately 1% of the mean value. In all cases the LII data correlated well with the standard surface area measurement techniques, exhibiting the correct trends with

changes in reactor operat
STSA (an established
illustrated in figure 17. V
the STSA data over the r

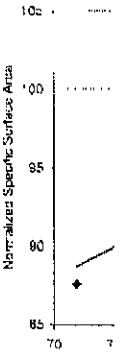

Figure 17. NSSA (a

4.6 Future Dev

A suite of high en
information about comb
techniques other than
quantitative measureme
Summaries of a number

By performing LI
measurements[31] interpret
aggregate theory,[55] chara
including size distribut
interest, assuming that th

The volatile fraction
laser-induced desorption
This technique uses two
stimulates laser-induced
sublimation of the soot,
light scattering is proport
pulse, of comparable en
remains, providing an el
volume of the remaining

ɔe expressed as

$$\frac{dI_p}{I} = \frac{6}{\rho_p D_{32}} \qquad (16)$$

and $p(d_p)$ is a probability
LII is proportional to the
D_{32} as

(17)

ter, 1.8 g/cm^3 is a typical
ssed in m^2/g. LII specific
wo carbon black reactor
qual to the independently
value at 100.

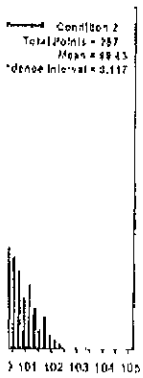

lack reactor conditions[43]

tions (NSSA) are shown
nfidence intervals on the
lth of the distributions of
, is approximately 1% of
d well with the standard
the correct trends with

changes in reactor operating conditions and a high degree of correlation with STSA (an established physical measure of specific surface area) as illustrated in figure 17. Variation in the LII data was significantly less than the STSA data over the range studied.[43]

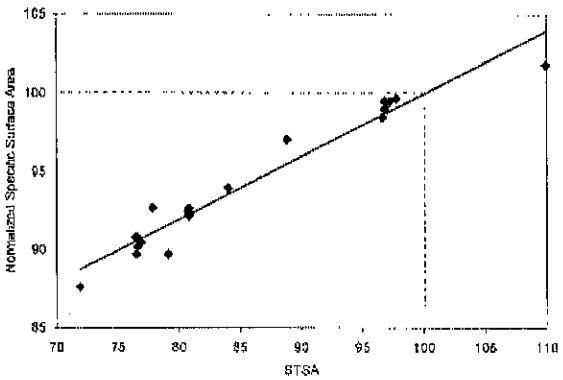

Figure 17. NSSA (as determined by LII) is highly correlated with STSA[43]

4.6 Future Developments

A suite of high energy laser diagnostics promises to offer detailed information about combustion generated particulate matter.[54] Currently the techniques other than LII are in their infancy in relation to making quantitative measurements of the properties of particulate emissions. Summaries of a number of these are presented below.

By performing LII and complementary elastic light scattering measurements[31] interpreted with Rayleigh-Debye-Gans polydisperse fractal aggregate theory,[55] characteristics of the aggregate size may be determined, including size distributions and other morphology-related properties of interest, assuming that the particles follow a log-normal distribution.[6]

The volatile fraction of PM can be measured in situ, in real-time with laser-induced desorption/elastic light scattering, a new optical diagnostic.[56] This technique uses two light pulses. The first pulse heats the particulates, stimulates laser-induced desorption of the volatile fraction without initiating sublimation of the soot, and scatters light from the particulates. This elastic light scattering is proportional to the total PM volume. The second laser light pulse, of comparable energy to the first, scatters light from the soot that remains, providing an elastically scattered signal that is proportional to the volume of the remaining solid portion of the PM. The ratio of the second to

the first measurements is then the quantitative solid volume fraction. Independent calibration would be required to obtain quantitative data for the volatile, solid, and total PM concentrations.

Laser-induced breakdown spectroscopy is a technique developed over the last two decades that has recently been applied to detect trace metal concentration in particulate matter.[57,58] A focused high fluence laser beam produces a spark at the probe volume, creates a plasma, dissociates molecules to elemental atoms, and excites the atoms. Atomic emission is produced as the atoms relax from the excited states, and spectra can be collected. The intensity of the atomic emission lines can be related to the concentration of the atomic species.

The combination of these techniques can provide *in-situ* real-time transient information about most aspects of particulate matter. Currently there is no complementary technique to provide information about the composition of the volatile organic fraction, which may be significant in terms of adverse health effects. However, encouraging developments may lead to success with the diagnostics discussed below.

Excimer laser fragmentation fluorescence spectroscopy can measure a number of chemical species at elevated temperatures with good sensitivity, selectivity, and time response, by focusing a UV pulsed laser beam to produce atoms or small fragments from larger compounds or particles that are normally non-fluorescing. It is showing promise in quantifying the relative concentrations of elemental carbon and volatile organic carbon.[59] It requires higher laser fluence than typically used with conventional LII (and much higher than with low fluence SC-LII), yet less than the fluence applied to generate a plasma in laser-induced breakdown spectroscopy.

Small-angle X-ray scattering has been applied to study the formation of soot spherules during fuel pyrolysis. These results have measured the mean diameters and dispersion of primary particles for a polydisperse distribution in the range from 1.6 to 35.0 nm.[60] A complementary technique is small-angle neutron scattering, which uses contrast variation to preferentially highlight or mask specific molecules, allowing identification of specific species.[61]

5. SUMMARY

Particulate characterization is extending beyond mere mass, equivalent sphere diameter, and qualitative measurements available in the past. With the emergence of these new optical diagnostic techniques, detailed *in-situ* transient real-time characterization of particulates is becoming possible. This

detailed characterization inc
concentration, soot tempere
volatile fraction, active s
distribution, and aggregate s
to provide particulate compo

These new capabilities ar
formation, growth, and o
emissions at the source; eva
understanding of the role of
opportunities for process
additional information prov
are now considering a broa
mass of particulates.

This new era of laser-ba
need for better characterizat
nanoscale particles such as
that novel methods, also ba
challenge.

ACKNOWLEDGEMI

The work at NRC C
Government's PERD Progr
supported by the NASA Gl
contracts and by the U.S. El

REFERENCES

1. C. Arden, R.T. Burnett, M.J
"Lung cancer, cardiopulmon
pollution." *Journal of the Am*
2. J. Hansen, M. Sato, R. Reto,
century: An alternative scen
9875-9880 (2000).
3. M.Z. Jacobson, "Strong rad
atmospheric aerosols," *Natu*
4. D.B. Kittelson, "Engines an
575-588 (1998).

e solid volume fraction.
in quantitative data for the

hnique developed over the
ed to detect trace metal
l high fluence laser beam
es a plasma, dissociates
toms. Atomic emission is
tates, and spectra can be
ines can be related to the

provide *in-situ* real-time
ticulate matter. Currently
le information about the
ich may be significant in
raging developments may
w.
ctroscopy can measure a
res with good sensitivity,
IV pulsed laser beam to
mpounds or particles that
omise in quantifying the
olatile organic carbon.[59] It
ith conventional LII (and
s than the fluence applied
pectroscopy.
to study the formation of
have measured the mean
polydisperse distribution
ntary technique is small-
ariation to preferentially
identification of specific

d mere mass, equivalent
ailable in the past. With
chniques, detailed *in-situ*
becoming possible. This

detailed characterization includes measurements of soot volume and mass concentration, soot temperature, total particulate concentration, solid-to-volatile fraction, active surface area, primary particle diameter and distribution, and aggregate size and distribution. Furthermore, developments to provide particulate composition appear promising.

These new capabilities are leading to: enhanced knowledge of particulate formation, growth, and oxidation; strategies for reducing particulate emissions at the source; evaluation of particulate filters and traps; improved understanding of the role of particulates in air quality and health; and new opportunities for process control in nanoparticle production. With the additional information provided by these laser-based techniques, regulators are now considering a broader range of measures than simply limiting the mass of particulates.

This new era of laser-based diagnostics has highlighted the longstanding need for better characterization of the optical and heat transfer properties of nanoscale particles such as soot and particulate matter, and it is anticipated that novel methods, also based on optical diagnostics, will arise to meet this challenge.

ACKNOWLEDGEMENTS

The work at NRC Canada was partially funded by the Canadian Government's PERD Program. The work of Artium Technologies, Inc. was supported by the NASA Glenn Research Center SBIR Phase I and Phase II contracts and by the U.S. EPA under SBIR Phase I contract.

REFERENCES

1. C. Arden, R.T. Burnett, M.J. Thun, E.E. Calle, D. Krewski, K. Ito, and G. D. Thurston, "Lung cancer, cardiopulmonary mortality, and long-term exposure to fine particulate air pollution," *Journal of the American Medical Association* **287**, 1132-1141 (2002).
2. J. Hansen, M. Sato, R. Reto, A. Lacis, and V. Oinas, "Global warming in the twenty-first century: An alternative scenario," *Proceedings of the National Academy of Sciences* **97**, 9875-9880 (2000).
3. M.Z. Jacobson, "Strong radiative heating due to the mixing state of black carbon in atmospheric aerosols," *Nature* **409**, 695-697 (2001).
4. D.B. Kittelson, "Engines and nanoparticles: A review," *Journal of Aerosol Science* **29**, 575-588 (1998).

5. P.O. Witze, "Diagnostics for the measurement of particulate matter emissions from reciprocating engines," *The Fifth International Symposium on Diagnostics and Modeling of Combustion in Internal Combustion Engines (COMODIA)*, Nagoya, 2001.
6. S.J. Harris and M.M. Maricq, "Signature size distributions for diesel and gasoline engine particulate matter," *Journal of Aerosol Science* **32**, 749-764 (2001).
7. G.J. Smallwood, D. Clavel, D. Gareau, R.A. Sawchuk, D.R. Snelling, P.O. Witze, B. Axelsson, W.D. Bachalo, and Ö.L. Gülder, "Concurrent quantitative laser-induced incandescence and SMPS measurements of EGR effects on particulate emissions from a TDI diesel engine," SAE Paper No. 2002-01-2715 (2002).
8. H. Zhao and N. Ladommatos, "Optical diagnostics for soot and temperature measurement in diesel engines," *Progress in Energy and Combustion Science* **24**, 221-255 (1998).
9. D.R. Snelling, G.J. Smallwood, R.A. Sawchuk, W.S. Neill, D. Gareau, W.L. Chippior, F. Liu, Ö.L. Gülder, and W.D. Bachalo, "Particulate matter measurements in a diesel engine exhaust by laser-induced incandescence and the standard gravimetric procedure," SAE Paper No. 1999-01-3653 (1999).
10. D.R. Snelling, G.J. Smallwood, Ö.L. Gülder, W.D. Bachalo, and S. Sankar, "Soot volume fraction characterization using the laser-induced incandescence detection method," *Proceedings of the 10th International Symposium on Applications of Laser Techniques to Fluid Mechanics*, Lisbon, July 10-13, 2000.
11. A.C. Eckbreth, "Effects of laser-modulated particulate incandescence on Raman scattering diagnostics," *Journal of Applied Physics* **48**, 4473-4479 (1977).
12. T. Ni, J.A. Pinson, S. Gupta, and R.J. Santoro, "Two-dimensional imaging of soot volume fraction by the use of laser-induced incandescence," *Applied Optics* **34**, 7083-7091 (1995).
13. J. Hult, A. Omrane, J. Nygren, C.F. Kaminski, B. Axelsson, R. Collin, P.-E. Bengtsson, and M. Aldén, "Quantitative three-dimensional imaging of soot volume fraction in turbulent non-premixed flames," *Experiments in Fluids* **33**, 265-269 (2002).
14. K. Kohse-Höinghaus and J.B. Jeffries, eds., *Applied combustion diagnostics*, Taylor and Francis, New York (2002).
15. L.A. Melton, "Soot diagnostics based on laser heating," *Applied Optics* **23**, 2201-2208 (1984).
16. C.J. Dasch, "New soot diagnostics in flames based on laser vaporization of soot," *Proceedings of the Twentieth Symposium (International) on Combustion*, 1231-1237 (1984).
17. N.P. Tait and D.A. Greenhalgh, "PLIF imaging of fuel fraction in practical devices and LII imaging of soot," *Berichte der Bunsengesellschaft fuer Physikalische Chemie* **97**, 1619-1625 (1993).
18. D.L. Hofeldt, "Real-time soot concentration measurement technique for engine exhaust streams," SAE Paper No. 930079 (1993).
19. B. Mewes and J.M. Seitzman, "Soot volume fraction and particle size measurements with laser-induced incandescence," *Applied Optics* **36**, 709-717 (1997).
20. D.R. Snelling, G.J. Smallwood, I.G. Campbell, J.E. Medlock, and Ö.L. Gülder, "Development and application of laser-induced incandescence (LII) as a diagnostic for soot particulate measurements," *Advanced Non-Intrusive Instrumentation for Propulsion Engines AGARD Conference Proceedings* **598**, 23.21 – 23.29 (1997).
21. K.R. McManus, J.H. Frai heated soot particles using
22. S. Will, S. Schraml, K. primary particle size m *Applied Optics* **37**, 5647-5
23. D.R. Snelling, F. Liu, G. heat and mass transfer i excitation intensity," Th NHTC2000-12132 (2000)
24. S. Schraml, S. Dankers measurements and implic LII)." *Combustion and Fl*
25. R.A. Dobbins and C.M. by thermophoretic sampli
26. W.H. Dalzell and A.F. S flux calculations," *Journa*
27. O. Leroy, J. Perrin, J. J surface and heat transfer 499-509 (1997).
28. G.J. Smallwood, D.R. Sn Errors in modeling laser- 814-818 (2001).
29. R.L. Vander Wal and K characterization towards 445-452 (1994).
30. C.R. Shaddix and K.C. production in steady and *Combustion and Flame* **1**
31. P.O. Witze, S. Hochgreb, laser-induced incandesce diffusion flame," *Applied*
32. C.J. Dasch, "One-dimens filtered backprojection m
33. D.R. Snelling, K.A. Thon imaging of soot volume 2485 (1999).
34. B. Quay, T.-W. Lee, T. volume fraction using las (1994).
35. R.L. Vander Wal, Z. Zhou gravimetric sampling." *C*
36. S. Schraml, S. Will, a concentration and primar resolved laser-induced in

iculate matter emissions from
n on Diagnostics and Modeling
IA), Nagoya, 2001.
s for diesel and gasoline engine
4 (2001).
D.R. Snelling, P.O. Witze, B.
ent quantitative laser-induced
on particulate emissions from a

t and temperature measurement
ience **24**, 221-255 (1998).
l, D. Garcau, W.L. Chippior, F.
neasurements in a diesel engine
d gravimetric procedure," SAE

achalo, and S. Sankar, "Soot
ced incandescence detection
ium on Applications of Laser

ite incandescence on Raman
73-4479 (1977).
-dimensional imaging of soot
ice," *Applied Optics* **34**, 7083-

on, R. Collin, P.-E. Bengtsson,
g of soot volume fraction in
, 265-269 (2002).
bustion diagnostics, Taylor and

Applied Optics **23**, 2201-2208

n laser vaporization of soot,"
l) on Combustion, 1231-1237

action in practical devices and
fuer Physikalische Chemie **97**,

d technique for engine exhaust

particle size measurements with
(1997).
Medlock, and Ö.L. Gülder,
cence (LII) as a diagnostic for
Instrumentation for Propulsion
.29 (1997).

21. K.R. McManus, J.H. Frank, M.G. Allen, and W.T. Rawlins, "Characterization of laser-heated soot particles using optical pyrometry," AIAA Paper No. 98-0159 (1998).
22. S. Will, S. Schraml, K. Bader, and A. Leipertz, "Performance characteristics of soot primary particle size measurements by time-resolved laser-induced incandescence," *Applied Optics* **37**, 5647-5658 (1998).
23. D.R. Snelling, F. Liu, G.J. Smallwood, and Ö.L. Gülder, "Evaluation of the nanoscale heat and mass transfer model of the laser-induced incandescence: Prediction of the excitation intensity," Thirty Fourth National Heat Transfer Conference Paper No. NHTC2000-12132 (2000).
24. S. Schraml, S. Dankers, K. Bader, S. Will, and A. Leipertz, "Soot temperature measurements and implications for time-resolved laser-induced incandescence (TIRE-LII)," *Combustion and Flame* **120**, 439-450 (2000).
25. R.A. Dobbins and C.M. Megaridis, "Morphology of flame-generated soot as determined by thermophoretic sampling," *Langmuir* **3**, 254-259 (1987).
26. W.H. Dalzell and A.F. Sarofim, "Optical constants of soot and their application to heat flux calculations," *Journal of Heat Transfer* **91**, 100-104 (1969).
27. O. Leroy, J. Perrin, J. Jolly, and M. Pealat, "Thermal accommodation of a gas on a surface and heat transfer in CVD and PECVD experiments," *Journal of Physics D* **30**, 499-509 (1997).
28. G.J. Smallwood, D.R. Snelling, F. Liu, and Ö.L. Gülder, "Clouds over soot evaporation: Errors in modeling laser-induced incandescence of soot," *Journal of Heat Transfer* **123**, 814-818 (2001).
29. R.L. Vander Wal and K.J. Weiland, "Laser-induced incandescence: Development and characterization towards a measurement of soot-volume fraction," *Applied Physics B* **59**, 445-452 (1994).
30. C.R. Shaddix and K.C. Smyth, "Laser-induced incandescence measurements of soot production in steady and flickering methane, propane, and ethylene diffusion flames," *Combustion and Flame* **107**, 418-452 (1996).
31. P.O. Witze, S. Hochgreb, D. Kayes, H.A. Michelsen, and C.R. Shaddix, "Time-resolved laser-induced incandescence and laser elastic scattering measurements in a propane diffusion flame," *Applied Optics* **40**, 2443-2452 (2001).
32. C.J. Dasch, "One-dimensional tomography: A comparison of abel, onion-peeling, and filtered backprojection methods.," *Applied Optics* **31**, 1146-1152 (1992).
33. D.R. Snelling, K.A. Thomson, G.J. Smallwood, and Ö.L. and Gülder, "Two-dimensional imaging of soot volume fraction in laminar diffusion flames," *Applied Optics* **38**, 2478-2485 (1999).
34. B. Quay, T.-W. Lee, T. Ni, and R.J. Santoro, "Spatially resolved measurements of soot volume fraction using laser-induced incandescence," *Combustion and Flame* **97**, 384-392 (1994).
35. R.L. Vander Wal, Z. Zhou, and M.Y. Choi, "Laser-induced incandescence calibration via gravimetric sampling," *Combustion and Flame* **105**, 462-470 (1996).
36. S. Schraml, S. Will, and A. Leipertz, "Simultaneous measurement of soot mass concentration and primary particle size in the exhaust of a DI diesel engine by time-resolved laser-induced incandescence (TIRE-LII)," SAE Paper No. 1999-01-0146 (1999).

37. S. Schraml, S. Will, A. Leipertz, T. Zens, and N. D'Alfonso, "Performance characteristics of TIRE-LII soot diagnostics in exhaust gases of diesel engines," SAE Paper No. 2000-01-2002 (2000).
38. S. Schraml, C. Heimgärtner, S. Will, A. Leipertz, and A. Hemm, "Application of a new soot sensor for exhaust emission control based on time resolved laser induced incandescence (TIRE-LII)," SAE Paper No. 2000-01-2864 (2000).
39. B.J. McCoy and C.Y. Cha, "Transport phenomena in the rarefied gas transition regime," *Chemical Engineering Science* **29**, 381-388 (1974).
40. R.L. Vander Wal, T.M. Ticich, and A.B. Stephens, "Optical and microscopy investigations of soot structure alterations by laser-induced incandescence," *Applied Physics B* **67**, 115-123 (1998).
41. D.R. Snelling, G.J. Smallwood, and Ö.L. Gülder, "Absolute light intensity measurements in laser-induced incandescence," US Patent No. 6,154,277 (2000).
42. D.R. Snelling, G.J. Smallwood, Ö.L. Gülder, F. Liu, and W.D. Bachalo, "A calibration-independent technique of measuring soot by laser-induced in-candescence using absolute light intensity," *The Second Joint Meeting of the US Sections of the Combustion Institute*, Oakland, California, March 25-28, 2001.
43. G.J. Smallwood, B.J. Stagg, and W.D. Bachalo, "Investigation of LII for online measurement of nanoparticle surface area in a carbon black reactor," *Twenty-Ninth Symposium (International) on Combustion*, WIP 3-1411, Sapporo, Japan, July 21-26, 2002.
44. S.S. Krishnan, K.-C. Lin, and G.M. Faeth, "Extinction and scattering properties of soot emitted from buoyant turbulent diffusion flames," *Journal of Heat Transfer* **123**, 331-339 (2001).
45. D.R. Snelling, K.A. Thomson, G.J. Smallwood, Ö.L. Gülder, E.J. Weckman, and R.A. Fraser, "Spectrally resolved measurement of flame radiation to determine soot temperature and concentration," *AIAA Journal* **40**, 1789-1795 (2002).
46. D.R. Snelling, F. Liu, G.J. Smallwood, and Ö.L. Gülder, "Determination of the soot absorption function and accommodation coefficient using low-fluence LII," *Twenty-Ninth Symposium (International) on Combustion*, WIP 3-1354, Sapporo, Japan, July 21 - 26, 2002.
47. M.E. Case and D.L. Hofeldt, "Soot mass concentration measurements in diesel engine exhaust using laser-induced incandescence," *Aerosol Science and Technology* **25**, 46-60 (1996).
48. G.J. Smallwood, D.R. Snelling, W.S. Neill, F. Liu, W.D. Bachalo, and Ö.L. Gülder, "Laser-induced incandescence measurements of particulate matter emissions in the exhaust of a diesel engine," *Proceedings of the Fifth International Symposium on Diagnostics and Modeling of Combustion in Internal Combustion Engines (COMODIA)*, Nagoya, 2001.
49. W.S. Neill, G.J. Smallwood, D.R. Snelling, R.A. Sawchuk, D. Clavel, D. Gareau, and W.L. Chippior, "Effect of EGR on heavy-duty diesel engine emissions characterized with laser-induced incandescence," *ASME-ICED 2002 Fall Technical Conference*, New Orleans, Sept. 8-11, 2002.

50. G.J. Smallwood, D.R. Snelli
L. Graham, "Transient parti
injection spark ignition auton
51. K. Schäfer, J. Heland, D.H. I
M. Birk, G. Wagner, P. Hase
K.J. Brockmann, V. Kriesch
R. Geatches, R. Burrows, J
measurements of aircraft e
intrusive techniques," *Applie*
52. M.G. Allen, B.L. Upschulte,
A. Hutchinson, D. Siveo, e
pollutant emissions from gas
53. T.P. Jenkins, J.L. Bartholo
Howard, "Laser induced inc
engine exhausts," AIAA Pap
54. P.O. Witze, "High-energy,
reciprocating engine PM emi
San Diego, August 25-29, 20
55. Ü.Ö. Köylü, "Quantitative
particle/aggregate parameter
emissivity," *Combustion ana*
56. P.O. Witze, "Real-time mea
using laser-induced desorpti
2002-01-1685 (2002).
57. R.L. Vander Wal, T.M. Tic
breakdown spectroscopy," *A*
58. M.-D. Cheng, "Real-time m
plasma techniques," *Fuel Pr*
59. C.B. Stipe, B.S. Higgins, E
using excimer laser fragmen
(International) on Combusti
60. J.P. Hessler, S. Seifert, and
studies of soot inception
Combustion, Sapporo, Japan
61. H. Wang, B. Zhao, B. Wys
soot formed in laminar
(International) on Combusti

N. D'Alfonso, "Performance
gases of diesel engines," SAE

. Hemm, "Application of a new
time resolved laser induced
4 (2000).
rarefied gas transition regime,"

as, "Optical and microscopy
luced incandescence," *Applied*

ite light intensity measurements
' (2000).
W.D. Bachalo, "A calibration-
l in-candescence using absolute
ons of the Combustion Institute,

vestigation of LII for online
black reactor," *Twenty-Ninth*
t, Sapporo, Japan, July 21-26,

nd scattering properties of soot
' of Heat Transfer **123**, 331-339

ülder, E.J. Weckman, and R.A.
radiation to determine soot
795 (2002).
er, "Determination of the soot
ng low-fluence LII," *Twenty-*
1354, Sapporo, Japan, July 21 -

measurements in diesel engine
nce and Technology **25**, 46-60

D. Bachalo, and Ö.L. Gülder,
late matter emissions in the
International Symposium on
bustion Engines (COMODIA),

uk, D. Clavel, D. Gareau, and
ic emissions characterized with
Technical Conference, New

50. G.J. Smallwood, D.R. Snelling, Ö.L. Gulder, D. Clavel, D. Gareau, R.A. Sawchuk, and L. Graham, "Transient particulate matter measurements from the exhaust of a direct injection spark ignition automobile," SAE Paper No. 2001-01-3581 (2001).
51. K. Schäfer, J. Heland, D.H. Lister, C.W. Wilson, R.J. Howes, R.S. Falk, E. Lindermeir, M. Birk, G. Wagner, P. Haschberger, M. Bernard, O. Legras, P. Wiesen, R. Kurtenbach, K.J. Brockmann, V. Kriesche, M. Hilton, G. Bishop, R. Clarke, J. Workman, M. Caola, R. Geatches, R. Burrows, J.D. Black, P. Hervé, and J. Vally, "Nonintrusive optical measurements of aircraft engine exhaust emissions and comparison with standard intrusive techniques," *Applied Optics* **39**, 441-454 (2000).
52. M.G. Allen, B.L. Upschulte, D.M. Sonnenfroh, W.T. Rawlins, C. Gmachl, F. Capasso, A. Hutchinson, D. Sivco, and A. Cho, "Infrared characterization of particulate and pollutant emissions from gas turbine combustors," AIAA Paper No. 2001-0789 (2001).
53. T.P. Jenkins, J.L. Bartholomew, P.A. DeBarber, P. Yang, J.M. Seitzman, and R.P. Howard, "Laser induced incandescence for soot concentration measurements in turbine engine exhausts," AIAA Paper No. 2002-0828 (2002).
54. P.O. Witze, "High-energy, pulsed laser diagnostics for real-time measurements of reciprocating engine PM emissions," *8th Diesel Engine Emissions Reduction Conference*, San Diego, August 25-29, 2002.
55. Ü.Ö. Köylü, "Quantitative analysis of in situ optical diagnostics for inferring particle/aggregate parameters in flames: Implications for soot surface growth and total emissivity," *Combustion and Flame* **109**, 488-500 (1996).
56. P.O. Witze, "Real-time measurement of the volatile fraction of diesel particulate matter using laser-induced desorption with elastic light scattering (LIDELS)," SAE Paper No. 2002-01-1685 (2002).
57. R.L. Vander Wal, T.M. Ticich, and J.R. West, "Trace metal detection by laser-induced breakdown spectroscopy," *Applied Spectroscopy* **53**, 1226-1236 (1999).
58. M.-D. Cheng, "Real-time measurement of trace metals on fine particles by laser-induced plasma techniques," *Fuel Processing Technology* **65/66**, 219-229 (2000).
59. C.B. Stipe, B.S. Higgins, D. Lucas, C.P. Koshland, and R.F. Sawyer, "Soot detection using excimer laser fragmentation fluorescence spectroscopy," *Twenty-Ninth Symposium (International) on Combustion*, Sapporo, Japan, July 21-26, 2002.
60. J.P. Hessler, S. Seifert, and R.E. Winans, "Spatially-resolved small-angle x-ray scattering studies of soot inception and growth," *Twenty-Ninth Symposium (International) on Combustion*, Sapporo, Japan, July 21-26, 2002.
61. H. Wang, B. Zhao, B. Wyslouzil, and K. Streletzky, "Small-angle neutron scattering of soot formed in laminar premixed ethylene flames," *Twenty-Ninth Symposium (International) on Combustion*, Sapporo, Japan, July 21-26, 2002.

Maria Clancy
National Research Council Canada
Inst For Chem Process & Envir Tech
M-12, Room 141, 1200 Montreal Rd.
Ottawa, ON K1A 0R6
CANADA

Telephone: 613/993-4041

Publication:	**OPTICAL METROLOGY FOR FLUIDS COMBUSTION AND SOLIDS**
Vol./Issue:	
Month/Year:	2003
Pages:	CHAPTER 8
Article Title:	PARTICULATE MEASUREMENT METHODS
Article Author:	
ISSN/ISBN:	
Series Title:	
Author:	SMALLWOOD GJ BACHALO WD AND SANKAR SV
Publisher:	
FAX/ARI:	
Max Cost:	
No/CI; Special Instr:	MARIA CLANCY;
Notes:	